Chapter

Principles of Membrane Surface Modification for Water Applications

Yilmaz Yurekli

Abstract

Membrane technologies offer efficient and reliable solutions to separate components from aqueous media. Among them, pressure driven membrane separation processes namely microfiltration (MF), ultrafiltration (UF), nanofiltration (NF) and reverse osmosis (RO) have been preferred in many industrial operations (food, pharmaceutical, chemical, drinking water, wastewater) due to the intrinsic advantages such as high selectivity, stability, ecocompatibility, scalability, flexibility, small footprint and low operational cost. This chapter will focus on the latest developments of surface modified polymeric membranes via the Layer-by-layer self-assembly approach and incorporation/decoration of nanomaterials. Variable parameters including size and charge of polyelectrolyte, ionic strength of the media, number of bilayers, and different types of nanomaterials on the bulk and surface property, water permeability, selectivity, antifouling, antibacterial, and adsorptive properties of the resultant composite membranes will be reviewed by comparison with the neat membranes. Membrane stability in terms of throughput and rejection characteristics during long-term filtrations will be addressed in this chapter.

Keywords: fouling, layer-by-layer self-assembly, membrane, nanometaloxide, surface modification

1. Introduction

The global water scarcity is one of the critical issues faced by human beings. Sustainability of the available water resources is very important for society's development which renders the transformation of wastewater into clean water is mandatory. One of the most challenges in the treatment of industrial and municipal wastewater is the quality and the corresponding cost of the treated water. Recent improvements in membrane technology have emerged as the most important and reliable treatment method for wastewater separation and recycling by the unique features including no need for chemical additives, thermal inputs, and spent media regeneration. The fact that the membrane market in the water and wastewater segment around the world is projected to reach USD 39.2 billion with a compound annual growth rate (CAGR) of 10.8% from 2013 to 2019 is a true indicator of this appeal [1]. Among different kinds of membrane materials, polymer-based membranes have the most common use owing to their relatively cheap manufacturing costs and simple fabrication processes [2, 3]. Polymeric UF, NF, and RO membranes

have been successfully used for the production of clean water and recent improvements have been summarized by Deng and Yin [4].

The hydrophobic nature of the polymeric membranes with their inherent permeability/selectivity trade-off is the most prominent problem that causes membrane fouling and lower throughput [5]. Applying one of the surface modification strategies (coating, grafting, blending, etc.) to convert surface non-polar groups into strong polar groups by the introduction of -OH, -COOH, $-NH_2$ has been accepted as a facile and robust way for the manufacturing of the membranes with desired hydrophilicity, leading to improved performance in terms of permeability, selectivity, and antifouling properties [6, 7]. It must be pointed out that the number of modification steps during the membrane fabrication process makes it difficult for large-scale production and the bulk structure of the membrane can be worse affected by the complex technological process, which will result in impairing the separation performance and mechanical strength of the membrane.

The LbL self-assembled surface modification via polyelectrolytes provides a defect-free ultra-thin surface accomplished on any negatively or positively charged surface by a single-step process. In addition, it is an environmentally benign process involving aqueous solution as the media at moderate temperatures. Another approach adopted to improve membrane performance is the impregnation/decoration of inorganic nanomaterials in/on the membrane. According to the literature, TiO_2, ZnO and Ag NPs [8–10] provide antibacterial, SiO_2 NPs [11] electrical conductance, carbon nanotubes (CNTs) such as single-walled CNTs (SWCNTs) and multi-walled CNTs (MWCNTs) [12] and graphene oxide (GO) [13] new water pathways, Fe catalytic property, and FeO NPs [14] magnetic property to the membrane. The hydrophilic nature of the nanomaterials with their high surface area to volume ratio, photocatalytic, antibacterial, and adsorptive capabilities have been widely utilized to modify the conventional polymeric membranes, aiming to overcome their limitations. For example, GO and TiO_2 nanoparticles have been attracted considerable attention, in which the former has abundant of oxygen-containing functional groups (e.g., carboxyl, carbonyl, epoxy groups, and hydroxyl), making them hydrophilic, hence improves membrane permeability [15], while the latter can contribute to continuous oxidation reactions, result in destruction or lethal effect on bacteria, virus, fungi, and algae [16, 17]. Zeolite nanoparticles with high ion exchange capability, on the other hand, add new functionality to the above-mentioned nanoparticles. Zeolites have well-defined porous structures and offer mobility of alkali and alkaline earth metals, in order to compensate net negative charge between Si4+ and Al3+ in the framework makes zeolites excellent adsorber for the removal of many target solutes [18–20]. The nanomaterials can be incorporated into polymer dope by physical blending [21] or deposited as a thin layer on the active layer of the membrane via layer-by-layer self-assembly [22], interfacial polymerization [23], surface grafting [24], or filtration [25, 26] methods.

In the following sections, recent developments in the fabrications and applications of membranes that meet the required throughput, selectivity, mechanical integrity, resistance to fouling, and low manufacturing cost will be discussed. Throughout the chapter, membrane modification techniques via layer-by-layer self-assembly and decoration/incorporation of inorganic nanoparticles (hybrid membranes) will be focused. The effect of variable parameters including size and charge of polyelectrolyte, ionic strength of the media, number of bilayers, and different types of nanomaterials on the bulk and surface property, water permeability, selectivity, antifouling, antibacterial, and adsorptive properties of the resultant composite membranes will be highlighted. Benefits and drawbacks of blending and coating methods will be discussed.

2. Surface modification strategies

This section focuses on the two methods commonly used for the modification of the surface properties of polymeric membranes. They are LbL self-assembly approach with and without inorganic nanoparticles, and surface decorated polyamid (PA) skin layer of thin film nanocomposite (TFN) membranes.

2.1 Surface modification based on LbL self-assembly

LbL self-assembly is a noninvasive method that does not impact the bulk properties of the supporting membranes. The superiority of this technique lies in the well-controlled of thickness, roughness, and charge of the layer. LbL uses polyelectrolytes which are normally hydrophilic and exhibit a charge. Chitosan, Polyethyleneimine (PEI), Poly(diallyldimethylammonium chloride) (PDADMAC), Poly(allylamine hydrochloride) (PAH) are extensively preferred cationic polyelectrolytes, while alginate, Poly(sodium 4-styrenesulfonate) (PSS), Sodium carboxymethyl cellulose are preferred as anionic polyelectrolytes [27, 28]. Deposition can be accomplished by alternating oppositely charged polyelectrolytes on support followed by rinsing after each step, which is used to remove excess and weakly adsorbed polyelectrolytes, hence defect-free ultra-thin layer around 2 nm is formed. A binary layer formed by two opposite polyelectrolyte deposits can be reproduced up to 60–100 multilayers [29, 30]. One of the coating processes including dip coating, spin coating or spray coating, which are schematically represented in **Figure 1** can be applied for LbL assembly. The main drawback of dip coating is the long process time due to diffusional resistance, and rinsing for the elimination of polyelectrolyte complex formation and hence flocculation on the surface. Successive deposition of highly ordered polyelectrolyte multilayers as a result of rapid rearrangement of polymer chains on the substrate is performed by a spin coating within a short time, however, the surface area of the material to be coated is limited. In the case of spray coating process, the polyelectrolyte solution is sprayed over a support membrane and the excess solution is drained by gravity. The processing time to finish deposition is almost two orders of magnitude lower than the dip-coating process and large surfaces can be easily coated with an automated spray coater.

The thickness and the morphology of the layers are influenced by the polyelectrolyte type, number of bilayers and deposition conditions (pH, salt concentration, polyelectrolyte concentration, and deposition temperature and time). For example, linear growth in the multilayer thicknesses was achieved for the PSS/PDADMAC system at 25 °C, while, the increase was reported exponential at 55 °C [32]. The number of sequential layered pairs is commonly known as to produce the thicker film, which corresponds to a lower permeability. However, according to Lajimi's results, the maximum flux, charge density, and hydrophilicity were observed when the number of CHI/ALG bilayers attained 15 [33]. This was explained by the transition of polyelectrolyte layers from a loose stratified structure to a tightened interpenetrating granular structure. In the following subsection, various parameters affecting the structure of the deposited layers will be discussed.

2.1.1 Factors affecting the structure of the LbL modified membranes

One of the most important parameters controlling the thickness, stability, and structure of layers is the salt concentration (ionic strength). Increasing ionic strength leads to thicker layers with a rougher surface [34]. The polyelectrolytes at high salt concentrations turn to coiled and loopy structures (instead of a flat

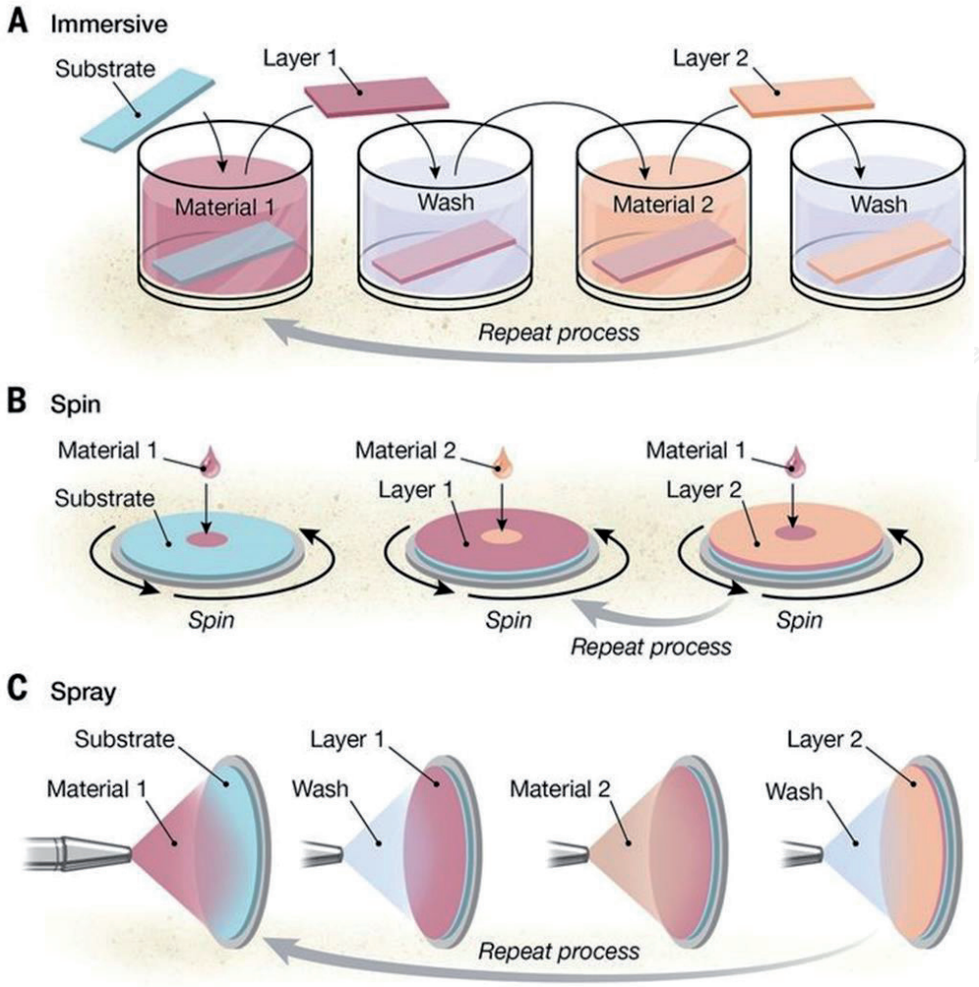

Figure 1.
Schematic representation of different processes used for LbL assembly: (A) dip coating, (B) spin coating and (C) spray coating. [31].

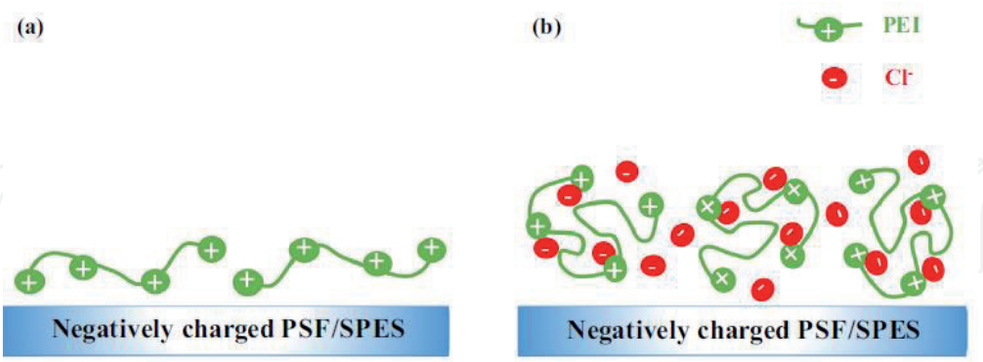

Figure 2.
Variation of the PEI deposition layer with respect to ionic strength of PEI solution. NaCl concentration in PEI solution (a) 0 M and (b) 0.5 M [35].

surface) with more charged chain segments, due to the screening effect, which prevents the electrostatic interaction between polyelectrolyte charges. This behavior is represented schematically in **Figure 2** [35]. In the presence of salt, more PEI adsorption occurs as a result of reduced segment/segment repulsions and increased surface/segment attractions. The reduction in repulsive forces between polyelectrolyte segments makes them small coils covering lower surface area per chain, causing to a larger area density of segments. The former is connected to the radius

of gyration (Rg), directly related to selectivity, while the latter is related to surface charge density. Tekinalp showed that the surface charge groups of PEI deposited layer in the presence of salt was higher compared to the salt free case. It has been also proposed that the first polyelectrolyte solution should contain a high concentration of salt, to improve surface segment interactions and thus higher polyelectrolyte adsorption, where a higher unbound charge can be used to form a stable and thin second layer. On the other hand, there is no need to add salt to the second polyelectrolyte solution in order to prevent the formation of thick and rough layers.

The strength of the interactions between polyelectrolyte layers, hence stability of the deposition is depended on the salt counterions which participate in charge neutralization called extrinsic compensation. The following ion exchange reaction can be used to explain this phenomenon [36]:

$$Pol^{+}Pol_{m}^{-}Na_{aq}^{+} + Cl_{aq}^{-} \leftrightarrow Pol^{+}Cl_{m}^{-} + Pol^{-}Na_{m}^{+} \tag{1}$$

$$K = \frac{y^{2}}{(1-y)[NaCl]} = \left(\frac{y^{2}}{[NaCl]_{aq}^{2}}\right)_{y\to 0} \tag{2}$$

where, m, K, and y represent deposited layers, equilibrium constant, and extrinsically compensated polyelectrolyte multilayers, respectively. High salt concentration results in an increased charge screening as the extrinsic charge overcompensation ($Pol^{+}Cl_{m}^{-}Pol^{-}Na_{m}^{+}$) is dominant over the intrinsic charge compensation ($Pol^{+}Pol_{m}^{-}$). At this condition, chains are more mobile due to the poor interactions between polyelectrolytes, which will enhance the possibility of layers detachment [37]. In fact, multilayer formation is thermodynamically favorable as the polyelectrolyte complexation has a small enthalpy change and increase in entropy [38]. The displacement of counterions when polyelectrolytes adsorb on an oppositely charged polyelectrolyte creates an increase in entropy. The sum of three terms determine the Gibbs free energy change of the LbL process. The first one, which is known as intrinsic compensation is the attraction energy carried out between surface charge groups and opposite charges on the polyelectrolyte. The second one, which is not desirable through LbL process is the conformational change caused by entropy loss. The third term is another penalty for deposition and is related to the segment/segment repulsive energy. It is clear that detachment of the deposited layers is prone when the sum of the repulsive and conformation energies exceeds the attraction energy. Therefore, charge density of polyelectrolytes and the ionic strength of the solution predominantly control the stability of the deposited multilayer. However, in some cases, where long-term usage under harsh condition of water purification, stability would be required to be increased, alternatively by using crosslinker between each polyelectrolyte layer [39].

Solution pH is another parameter influencing the morphology of the deposited layer. Thicker layer forms during polyelectrolyte assembly carried out at a high pH. Thin layers with flat chain conformations are attained in the case of highly charged polyelectrolytes. Polyelectrolytes at high pH are partially ionized and incorporating more nonionized chain segments is prone to swell. Therefore, the solution pH determines the charge density of polyelectrolytes, hence surface charge density. At the deposition pH corresponding to the average of the pKa values of the polycation and polyanion, maximum density of ionic cross-links in the assembly is achieved. Unless the charge density is below a minimum value the charge reversal is possible for the formation of multilayers [40].

In order to overcompensate surface charges, charge density and polyelectrolyte concentration in dipping solution should be high. Temperature selected during polyelectrolyte assembly influences the final structure of the film. Higher temperature results in thicker layer due to the chain mobility leading to an increase in the number of loops and tails adsorbed to the membrane surface. The molecular weight of polyelectrolyte influences the stability of the deposited layer. Wang et al. studied the impact of molecular weight of cationic PEI on the permeability and rejection performance of the hydrolyzed PAN membrane [41]. 3.5 bilayers were established by keeping the molecular weight of sulfonated poly (ether ether ketone) constant, which was selected as an anionic polyelectrolyte. Water fluxes with the increase in layers were decreased for both high (25,000) and low (800) molecular weight PEI, however, no salt rejected in the case of low molecular weight PEI was observed. This was explained by the lower structure of the selective layer. Consequently, when using low molecular weight PEI, a higher number of layers could be necessary to achieve salt rejection. The support membrane is, on the other hand, limited to the first few bilayer depositions. Surface charge density and the relative dielectric permittivity of the support may alter the morphology of the multilayer assembly up to a thickness in the micrometer range [42]. In general, a good support membrane for the LbL assembly is expected to have a low surface roughness and a high surface charge density.

2.2 Surface modification containing nanomaterials (TFN)

The purpose of the surface modification of membranes used in water treatments is to reduce or eliminate fouling, which is the main problem in any membrane separation process. In the NF processes, the starting material is usually selected as UF membrane. The polyamide thin film composite (TFC-PA) membranes have been successfully used in water treatment for the purpose of desalination and decolorization, however, membrane fouling and chlorine intolerance cause to decline the permeation flux, shorten the service life, and increase the operating cost, and hence reduce the long term process efficiency. Therefore, researches based on nanoparticle decorations in a skin layer of the asymmetric membrane for NF applications have been rapidly increased.

In TFC-PA approach, nanoparticles are introduced either in organic or aqueous phase. However, the hydrophilic nature of the mostly inorganic nanomaterials necessitates their use in aqueous amine solution. Interfacial polymerization (IP) occurs as soon as acyl and amine monomers interact with each other, in which nanoparticles are either embedded within the polymer matrix or dispersed on top of the polymer film depending on the approach of introducing nanoparticles. The so-called membrane is typically rinsed with hexane or water followed by heat treatment to complete polymerization.

Carbon nanotube (CNT) has intensively attracted attention due to high aspect ratio, low density, mechanical strength, and stiffness. However, its hydrophobic nature makes dispersion problems in various solvents (NMP, DMAc, DMSO, DMF) as well as within a polymer matrix. Therefore, many efforts have been focused on introducing hydrophilic/functional moieties or macromolecules on a CNT surface [43]. Various methods, including acid treatments, plasma oxidation, chemical grafting, in situ polymerization, amination, hydrothermal treatment, and TiCl4 precipitation on the acid treated multi-walled carbon nanotube (MWCNT) have been successfully investigated for the addition of functional groups such as carboxylic, amine, hydroxyl etc.

MWCNT-NH_2 has been embedded in PA layer to improve separation performance of the NF membrane. Dispersion of 0.001 to 0.01 w% MWCNT-NH_2 in

piperazine monomer solution followed by the interfacial polymerization revealed that the MWCNT-NH_2 was successfully dispersed within the PA layer, and the modified NF membranes had high hydrophilicity, smoothness, enhanced separation performance, and antifouling property [44]. Similarly, Xue et al. studied the effect of MWCNTs with different functional groups (MWCNT–COOH, MWCNT–OH, or MWCNT–NH) on the NF performances [45]. Piperazine solution consisting of 1 w% functionalized CNT was cast on PSf UF membrane. The coated membranes were than immersed into an organic acyl solution to initiate interfacial polymerization. The remarkable results for thin film nanocomposite NF membranes obtained from different fabrication approaches are summarized in **Table 1**.

Wu et al. used MF membrane to fabricate NF by vacuum filtration of functionalized CNT suspension followed by IP process [55]. The thickness and roughness of the intermediate layer determined the PA active layer morphology. Authors observed that the thickness of the active layer was increased with an increase of CNT layer which associated with the absorbed monomer on the coated membrane. Remarkable results from CNT loaded UF and NF membranes have been summarized in literature [43].

GO is another carbon-based nanomaterial, which has charged oxygen-containing functional groups. Owing to its laminar structures with high surface area, GO nanosheet is mostly preferred for MF, UF membrane surface modification via vacuum filtration or LbL assembly methods. The number of deposition cycles can adjust the thickness of GO layer at a molecular level. Thin layer formation occurs based on alternatively depositing polyelectrolytes and GO nanosheets through

Substrate	Method	Nanofiller	Remarkable features	Ref.
PSf	IP (PIP-TMC)	Modified SiO_2 NPs (100 nm)	Enhanced fouling resistance, long term stability and proper pore size	[46]
PSf	IP (TMC-MPD)	Biocidal GO nanosheets	Good bacterial inactivation without alteration intrinsic transport properties of the membrane	[47]
PSf	IP (TMC-MPD)	GO nanosheets	Enhanced water permeability	[48]
PES	IP (PIP-TMC)	ZIF 8/GO hybrid nanosheets	High antibacterial activity and salt retention	[49]
PES	PVA coating layer	TiO_2	Enhanced water flux and NaCl salt rejection	[50]
PAN	PEI-g-GA coating layer		Impressive prospect for the dye reuse	[51]
PES	Chitosan incorporated GO coating layer		High antibacterial activity	[52]
PP (MF)	LbL (CMCNa- PEI) crosslinked with GA		Highly potential to the application of dye removal and partial desalination with high permeability.	[53]
PVDF	Vacuum filtration	LDH@g-C3N4@ PDA/GO	Superior dye rejections, water flux, and photocatalytic self-cleaning ability	[54]

Table 1.
Thin film nanocomposite NF membranes fabricated by using different approaches and their performance summary.

electrostatic attractions. Zhao et al. fabricated ultrathin hybrid membranes via LbL self-assembly using gelatin (GE) and GO on hydrolyzed PAN membrane [56]. The positively charged GE interacted with negatively charged GO in the self-assembly process, leading to efficient multilayers.

Song et al. functionalized and anchored GO nanosheets with polyelectrolyte to further enhance the separation performance of the GO membranes [57]. GO modification was carried out with ethylenediamine (EDA) molecules, followed by poly (allylamine hydrochloride) (PAH) anchoring to amplify the surface charge density. Amine reduced GO (ArGO) anchored by PAH (PAH@ArGO) nanosheets with positive charge and PSS@GO nanosheets with negative charge were alternately deposited on the polycarbonate support via LbL assemblyThe selective layer thickness of the PE@ArGO membrane was about 160 nm, possessed high density positive/negative charge gated ion transport nanochannels and superior salt rejection by means of Donnan charge exclusion.

However, instability of GO (disintegration or re-dispersion) in water is one biggest block that limits its practical usage. Covalent crosslinking is a promising strategy for the solution of this problem. The functional groups on the GO nanosheets such as hydroxyl and carboxyl groups are convenient sites for the cross-linking reaction with different crosslinker. Mie et al. fabricated a GO membrane covalently cross-linked by 1,3,5- benzenetricarbonyl trichloride between acyl chloride and carboxyl groups [58]. Results revealed that cross-linking effectively ensured the GO membrane with necessary stability to prevent its inherent dispensability in an aqueous environment.

MOFs are porous crystalline materials possess superior compatibility in polymer matrix, apart from other inorganic nanomaterials. By their unique features including size, shape, and polarity, MOFs provide preferential passage for certain molecules, simultaneously rejected undesired substances, when embedded in membrane phase. Gong et al. prepared positively charged NF membrane by incorporating NH2-MIL-125(Ti) porous titanium based MOFs material into PEI and trimesic acid (TMA) crosslinking system [59]. The structure and the experimental procedure are illustrated in **Figure 3(1a-c** and **2)**. The effect of MOFs loading amount on the NF

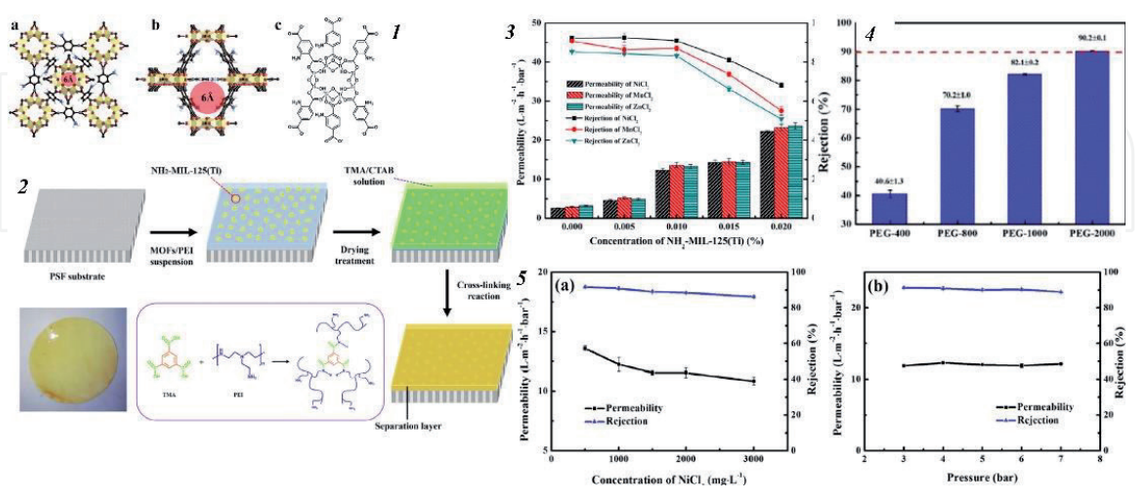

Figure 3.
(1) (a, b) Schematic of NH2-MIL-125(Ti) structure (H, white; C, black; O, red; N, blue; Ti, yellow polyhedral) and (c) the structural formula of NH2-MIL-125(Ti), (2) Schematic of the preparation of NH2-MIL-125(Ti)/PEI/TMA composite membranes, (3) The effect of NH2-MIL-125(Ti) loading on heavy metal removal performance of NH2-MIL-125(Ti)/PEI/TMA composite membranes, (4) Selectivity of different PEG solutions (pressure: 4 bar; solute concentration: 200 mg/L) by the MPT-0.010 composite membrane, (5) Heavy metal (Ni2+) removal performance of the MPT-0.010 composite membrane at different (a) feed concentrations (test pressure: 4 bar) and (b) test pressures (salt concentration: 1000 mg/L) [59].

performance, metal rejection, and stability were studied. The surface roughness of the membrane increased from 6.9 to 92.4 nm when the MOFs loading increased from 0.0 to 0.02 w%. The rejection of Ni^{2+}, Mn^{2+}, Zn^{2+} and permeability optima was obtained, at 0.01 w% of MOFs (**Figure 3 (3)**). Beyond this value, metal rejections reduced seriously. The MWCO of the membrane based on 90% or above PEG rejection (**Figure 3 (4)**) showed that the composite membrane could be considered as a loose NF membrane having an effective pore radius and PEG rejection of 1.5–2.2 nm and 1000–2000 Da, respectively. Furthermore, the resultant composite membrane was found to be positively charged over a large pH interval (3–11) that could be ascribed to the protonation of amine groups. The increase in hydraulic permeability, while maintaining with similar rejection by the introduction of MOFs was attributed to the preferential water channels and suitable window size, that can selectively cut off heavy metal ions allowing water molecules to pass through. In addition, the positive surface charge density of the nanocomposite membrane contributed to the rejection of heavy metal cations by electrostatic repulsive forces.

3. Blending method

The introduction of inorganic nanomaterials (eg. TiO_2, ZnO, GO, Al_2O_3, and SiO_2) into polymer dope to make mixed matrix membrane (MMM) has been favored over the other methods including coating and grafting due to its simplicity. These nanoparticles are attractive in wastewater treatment, because of their porous textures, high surface area to volume ratio, high pore volume and their surface functional groups (-OH) which impart enhanced hydrophilicity and surface properties of the resultant membranes. They form new water pathways, increase solute rejection and control the degree of fouling.

MMM can be configured in both flat sheet and hollow fiber forms based on phase inversion process. Homogenous solution is prepared by dispersing the nanomaterials in a suitable organic solvent (N-methyl-2-pyrrolidone, dimethylformamide, dimethylsulfoxide, dimethylacetamide). A certain amount of polyethyleneglycol or polyvinylpyrrolidone as pore former is introduced to the solution. After sonication, the suspension is slowly added into the main membrane forming material (PSf, PAN, PWDF etc.). The dope solution is continuously stirred overnight, followed by casting process with the required thickness. An asymmetric membrane is then produced by placing the composite film into coagulation bath for nonsolvent induced phase inversion. The incorporation of the inorganic nanoparticles alter the bulk structure of the membrane as they hinder the interaction between polymer and solvent molecules [60]. Their hydrophilic character changes the solvent exchange rate during phase inversion process leading to a thin and dense selective layer with a finger like support layer. The hydrophilic nature of the nanoparticles causes them to move towards the surface during phase inversion process. This enhances the surface properties of the resultant membrane.

3.1 Nanocomposite membranes prepared by blending method

The research in improving the properties of nanofiltration membranes is recently increased tremendously. Various nanomaterials including GO, CNT, metal organic frameworks (MOF) (ZIF-8), TiO_2, SiO_2, zeolite, have been incorporated to form a nanocomposite membrane with high performance. In the following part, a review will be provided to highlight the performance of these composite membranes.

3.1.1 Metal organic frameworks

MOFs consist of metal ions or clusters coordinated to organic ligands to form 1D, 2D or 3D structures. High crystallinity, porosity (up to 90%), internal surface areas (over 6000 m^2/g), and stability make MOF ideal candidate for the enhancement of the membrane performance. The possibility of synthesizing different structures having various sizes and functionalities for a specific application is another advantageous of the MOFs [61]. This is important, since the main problem encountered during incorporation of inorganic nanomaterials into polymeric matrix is their incompatibilities [62]. Filler-polymer compatibility can be improved by the organic constituents of MOFs.

Ze-Xian Low studied the effect of 2D ZIF-L nanoflakes on the performance of the PES UF membrane [63]. Incorporation of ZIF-L was significantly improved water flux without greatly altering the MWCO of the modified UF membrane. Similarly, the combined effect of lower surface roughness, zeta potential, and higher hydrophilicity, caused to a lower bovine serum albumin (BSA) attachment onto the surface of the composite membrane. With those outstanding features, fouling resistance of the so-called membrane against BSA enhanced almost twice with more than 80% flux recovery.

In literature, MOF type materials have been extensively studied in heavy metals adsorption as they provide tunable pores and high specific area [64, 65]. The adsorptive characteristics of UiO-66-NH2 MOF has been tested by incorporating into PAN/CHI dope solution to make composite nanofiber [66]. The adsorptive membrane incorporated with 10 w% of UiO-66-NH2 MOF showed maximum monolayer coverage of 441.2, 415.6, and 372.6 mg/g for Pb^{2+}, Cd^{2+}, and Cr^{6+}, respectively, in static condition. In crossflow filtration, carried out 20 mg/L initial metal concentration at 1 bar TMP, the permeation flux and metal removal were observed as for 452, 463, and 479 L/m^2.h., and 94, 89, and 86%, respectively for Pb^{2+}, Cd^{2+}, and Cr^{6+}. During long term filtration, slightly reduced permeation flux and rejection were obtained up to 18 h., beyond this point, a significant reduction in both flux and rejection revealed that the nanofibrous membrane pores were saturated.

3.1.2 Zeolite NPs

Zeolite nanoparticles with their unique properties such as high ion exchange capacity and fast adsorption rate make it excellent choice for the separation of heavy metals in wastewater treatment [67] and desalination process [68]. In the study of Yurekli, variations in the morphologies and the filtration performances of the zeolite NPs blended PSf hybrid membranes have been investigated with respect to the loading amount of zeolite NPs [67]. **Figure 1** indicates surface and cross-sectional SEM microphotographs of the native and zeolite NPs incorporated PSf membranes. Formation of the new pores with larger diameters in **Figure 4** has been attributed to the phase separation occurred quickly and to the aggregation of the NPs. Compared to the native PSf membrane, zeolite loaded PSf membrane has more uniformly distributed finger-like pores which are extended through the thickness of the membrane that shortens the pathway (tortuosity) of the solutes, hence improve the hydraulic permeability. An increase in the hydraulic permeability value of 94% for the PSf10–30 membrane has been attained compared to the pristine PSf (23.2 L/m2.h.bar). It was observed that the retention of heavy metals through the PSf10–30 membrane was more pronounced at lower transmembrane pressures and heavy metals concentrations.

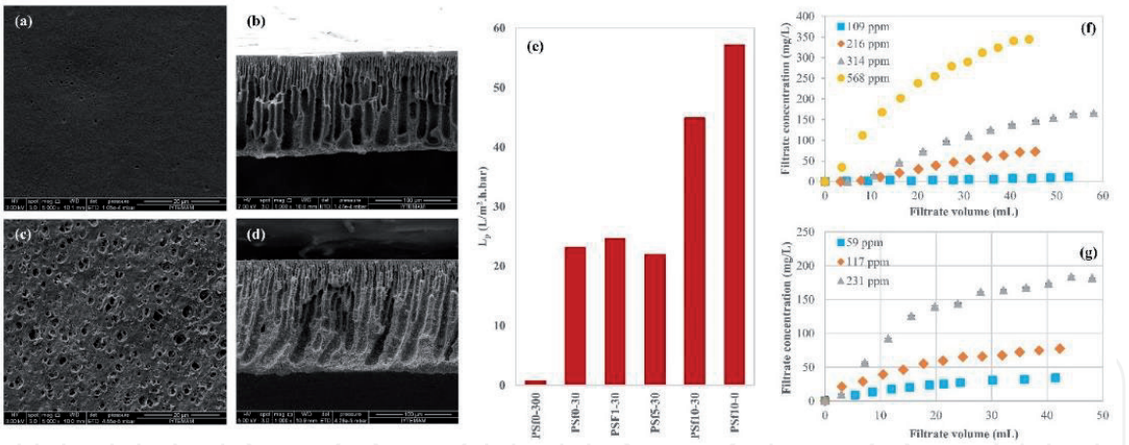

Figure 4.
SEM microphotographs of the native and zeolite incorporated PSf membranes; (a, c) top surface and (b, d) cross-sectional images of the native and 10% zeolite added PSf membranes, (e) hydraulic permeabilities of the PSf membranes prepared with different amount of zeolite NPs, (f) Pb2+ and (g) Ni2+ concentrations in permeate during filtrations of Pb2+ or Ni2+ aqueous solutions, respectively in different initial concentrations through PSf 10–30 membrane at 1 bar. [67].

3.1.3 GO NPs

Similarly, Mukherjee et al. studied the impact of GO NPs on the removal of heavy metals using mixed matrix membrane (MMM) [69]. GO NPs were synthesized based on the modified Hummer method, blended in different fractions with PSf dope solution and prepared the MMM by phase inversion method. The main results extracted from the study of Mukherjee is depicted in **Figure 5**. From **Figure 5(a)-(c)** addition of GO NPs into PSf matrix increased MWCO, porosity, negative charge density, and permeability of the MMM. Based on the preliminary cross-flow tests 414 kPa was selected as optimum TMP considering both rejection and permeabilities of the membrane. In order to investigate reusability of the MMM, the fouled membrane with 50 mg/L chromium aqueous solution

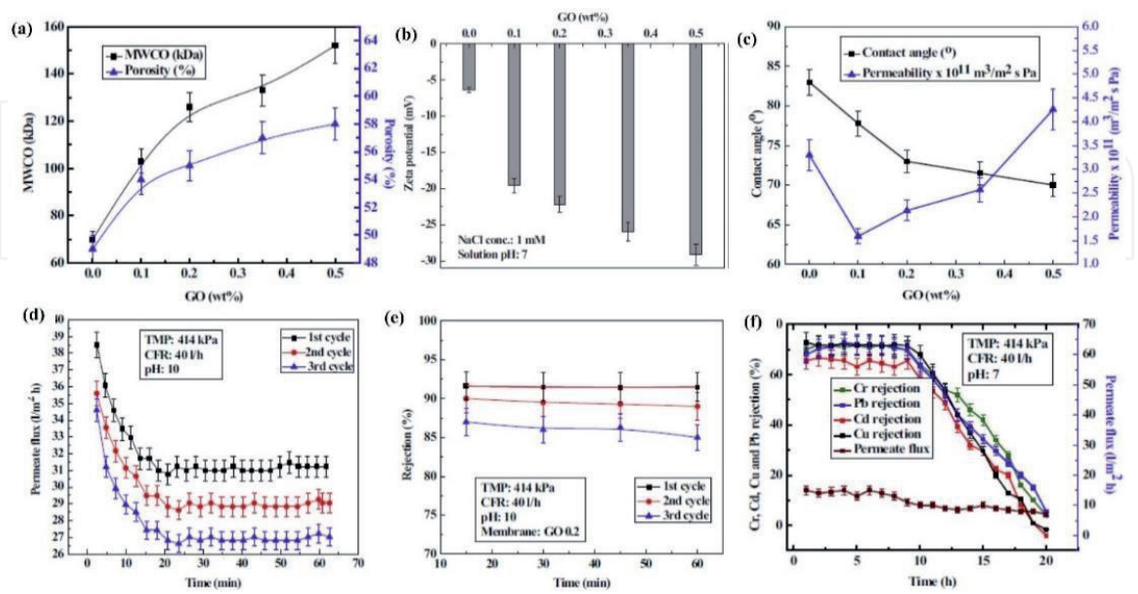

Figure 5.
Effect of GO concentration on (a) MWCO and porosity; (b) zeta potential at neutral pH (c) contact angle and permeability. Effect of regeneration on (d) permeate flux and (e) rejection by GO 0.2 membrane, with 414 kPa TMP, 40 l/h CFR and operated at pH 10. (f) Long duration filtration performance of GO 0.2 membrane in case of filtration of mixed metal solution at 414 kPa TMP and 40 L/h CFR. [69].

in cross-flow mode of 414 kPa and 20 L/h of retentate flow rate for 1 hour was washed first with water for 10 min and then with acidic solution at pH 5.5 for 30 min and again with water to remove all the acidic residuals. All the steps in the regeneration cycle were carried out in dynamic conditions similar to the case in fouling. The reduction in solution flux at each cycle was explained as the accumulation of chromium ion at the GO surface, which was also observed by the reduction in rejection values in the consecutive cycles (**Figure 5(a)** and **(b)**). The results from long term filtration performance of the MMM with respect to the mixed metal solution (Cr, Cu, Cd, and Pb) each having concentrations of 50 mg/L, as illustrated in **Figure 5(f)** demonstrated the permeate flux decreased continuously. The authors concluded that the simultaneous adsorption of different heavy metals, on the membrane increased the resistance of adsorption, which resulted in permeate flux reduction rapidly with time. Finally, the concentrations of all heavy metals in permeate remained almost constant up to breakthrough time (8 h) and increased thereafter till feed concentration.

3.1.4 TNT nanotubes

Subramaniam et al. fabricated PVDF hollow fiber UF membrane incorporated with titanate nanotubes (TNTs) for decolourization of aerobically-treated palm oil mill effluent [70]. TNTs which were synthesized based on the alkaline hydrothermal process were dispersed in NMP under sonication for 30 min. Hollow fiber membranes were fabricated by means of a dry-jet wet spinning method by changing the amount of TNTs in the bore solution of TNT/PVP/PVDF in between 0–1%. The spherical TiO_2 nanoparticles were reported to be converted into completely TNTs with an average diameter of 24 nm at the end of the hydrothermal process. The variation in the pore size was more pronounced by the addition of pore former than the addition of TNT into the dope solution meaning that the addition of TNT had no considerable effect on the pore size and finger-like structure of the membrane. The result was evidenced by the similar porosity values obtained for all the membrane formulations. Addition of TNT increased the membrane roughness, BSA rejection, color rejection and water flux simultaneously (**Figure 6a**). However, beyond a certain amount of TNT loading, a reduction in water flux has been observed, which was ascribed to the aggregation of NPs. The authors finally investigated the flux recovery and antifouling performances of the resultant membranes during 5 regeneration cycles as depicted in **Figure 6**. Regeneration was accomplished by first fouled the membrane with AT-POME at 1 bar for 240 min using cross-flow filtration, then the fouled membrane was washed with water for 30 min. In **Figure 6**, the fluxes in all membrane configurations decreased over time but the flux recoveries for all the membranes after 5 cycles were observed above 80% except the pristine PVDF, which exhibited gradual declination of flux throughout the test. Similarly, all the membranes comprised of TNT regardless of loading were able to recover rejection performance after water washing

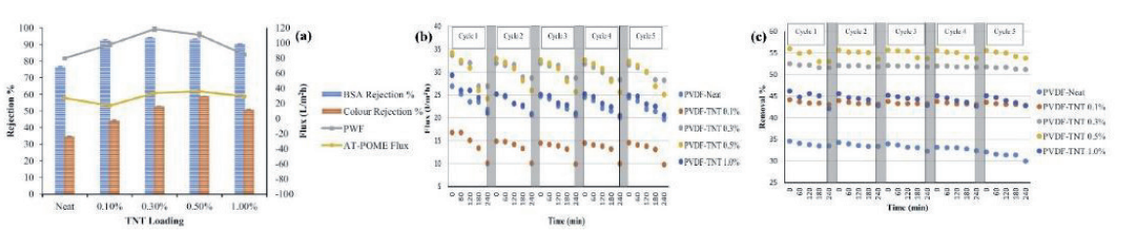

Figure 6.
(a) Pure water fluxes, AT-POME flux, BSA and color removal (b) AT-POME flux and (c) AT-POME color removal for five cycles of AT-POME filtration [70].

but pristine PVDF showed declining rejection through 5 cycles. The results has been related to the variation of the hydrophilic natures of the membranes.

3.1.5 Alumina NPs

Alumina NPs loaded PVDF membrane fabricated according to the phase inversion method has been demonstrated that the hydrophilicity, permeability, antifouling capacity, and mechanical stability were increased with no considerable change in pore density and size [71]. In another study, fouling resistive, reduced flux decline and less hydrophobic interaction between foulant and membrane surface are some of the outstanding features of the alumina NPs added PES UF membrane [72]. Different types of NPs have been incorporated into variable polymeric matrix to improve separation performances and fouling resistance of the hybrid membranes and their characteristics compared to the pristine ones collected from recently published studies have been listed in **Table 2**.

Nanoparticles used to fabricate a hybrid membrane can also enhance the mechanical stability compared to the pristine membrane by decreasing the impact of the membrane compaction. Compaction is known as the mechanical deformation of the polymeric membrane matrix and observed at the initial stage of the pressure driven membrane operations. Structure densification leads to a flux decline. Blending NPs with polymer matrix allows well distribution of NPs through the thickness of the membrane during phase inversion process. The stability of those NPs in the macrovoid region reduces the loss of membrane structure because compaction is known to occur predominantly in bulk macrovoid region. For instance, Pendergast et al. reported that stability of PSf membranes was improved when silica and zeolite NPs were included in the membrane structure, resulting in less compaction than pure PSf membrane [86].

3.1.6 Surface modified NPs

Although, the addition of the NPs into polymer matrix by simple blending method offers superior advantageous in terms of rejection, antifouling, and permeability, the tendency of NPs to agglomeration due to high surface free energy and high affinity to water molecules during phase separation on one hand, and the possibly release of NPs into filtrate due to weak interactions between NPs and polymer chains on the other hand, makes surface modification of NPs mandatory to obtain a hybrid membrane with well dispersed, stable, and compatable NPs. Modifications are based on either chemical treatment of NPs or grafting of functional polymers on hydroxyl groups available in NPs. Oxidation, for example, could be the desired pathway through acid treatment to create carboxyl and hydroxyl functional groups on carbon nanotubes. Different surfactants have also been proposed to be grafted on NPs surfaces to mitigate the agglomeration and their mechanisms have been reviewed detailed in the literature [87]. Besides the improvement of homogenous dispersivity, stability, and compatibility, the functionalization of NPs increases the membrane antifouling property as they offer higher surface charge density, which is useful for the rejection of the foulants. Ayyaru and Ahn studied with the PES nanocomposite membranes blended with surface modified TiO_2 NPs (anatase, 20–25 nm in size) for fouling mitigation [88]. The TiO_2 nanoparticles were sulfonated by replacing the surface hydroxyl groups with $–SO_3H$ group and the loading effect of $sTiO_2$ NPs was investigated. Surface roughness, porosity, and pore size of the modified membranes exhibited notable enhancement compared to the PES membrane. Increasing porosity revealed a good distribution of $sTiO_2$ NPs in the dope solution. The improved properties of $sTiO_2$ blended membranes such as high hydrophilicity permeability, anti-fouling performance, and improved BSA rejection were attributed

Polymer	Filler	Method	CA (°)	Foulant	The main contributions of nanoparticles to the resultant membrane	Ref.
PES	TMU-5 MOF	NIPS	67.2–51.6	8000 ppm powder milk solution	Hydraulic permeability increased from 44.4 to 60.7 L/m2.h.bar. Surface become smoother (roughness reduced from 43.9 to 5.2 nm.) and flux recovery ratio (FRR) increased to 25.5 to 98.7%. After 5 cycles 99% of water flux recovery was obtained.	[73]
PVDF	CNT/GO	NIPS	79.6–62.1	1000 ppm BSA solution	Hydraulic permeability increased from 75.5 to 125.6 L/m2.h.bar. Pore size after nanoparticle addition increased from 14.5 to 18.5 nm. Roughness exceptionally increased from 12.9 to 30.9 nm. FRR increased from 52 to 60.6%.	[74]
PVDF	Amine functionalized silica	Dip coating	66–32	Mixture of organic and inorganic foulants	The addition of nanoparticles improved pore size (30.4 to 50.3 nm.) and water permeability (648 to1512 L/m2.h.bar) of the resultant membrane. No significant change in roughness was observed and FRR improved from 53 to 80%.	[75]
PSf	Cuprous iodide nanosheets	NIPS	71.6–60.4	500 ppm BSA solution (pH 7.3)	The increase in pore size (from 58.2 to 92 nm.) and hydrophilicity resulted in an increase in hydraulic permeability (556 to 1473 L/m2.h.bar). FRR value was slightly improved (31–36%). At the end of 6 regeneration cycles 36% water flux recovered.	[76]
PES (MF)	CuO NPs	NIPS	69.8–64	500 ppm BSA solution	Hydraulic permeability increased from 266 to 435 L/m^2.h.bar. Pore size after nanoparticle addition increased from 13.9 to 17.8 nm. Surface roughness reduced from 3.2 to 2.5 nm. FRR was slightly improved from 45.5 to 48.2%.	[77]
CA (UF)	GO/MOF@GO	NIPS	73.2–49.5	1000 ppm BSA solution	Both rejection (91.4–95.4%) and hydraulic permeability (66–122 L/m^2.h.bar) enhanced. The reduction in surface roughness from 25.2 to 7.2 nm. caused to increase FRR from 49.8 to 88.1%.	[78]
PVDF (UF)	AC/TiO_2	NIPS	80.4–66.4	20 ppm HA solution	Pore size (18 nm.), surface roughness (22.4 nm.) values were unchanged, but hydraulic permeability improved from 90 to 172 L/m^2.h.bar. FRR was reduced from 90.6 to 83.3%, due to strong interaction of the foulants with AC. After 2 regeneration cycles 87% of water flux was recovered.	[79]
PSf (UF)	GO/CGO	NIPS	90.6–73.1	1000 ppm BSA solution	Hydraulic permeability increased from 60 to 123 L/m^2.h.bar with a rejection value of BSA larger than 99.5%. Smoother surface (reduction in surface roughness from60.7 to 23.1 nm.) and lower FRR value (from 68.6 to 52.7%) were reported.	[80]

Polymer	Filler	Method	CA (°)	Foulant	The main contributions of nanoparticles to the resultant membrane	Ref.
PES (UF)	HANTs	NIPS	83.6–67.1	1000 ppm BSA solution pH 7.4	Addition of nanoparticles caused all pore size (34.1–43.2 nm.), surface roughness (10–19.4 nm.), hydraulic permeability (169–439 L/m^2.h.bar), and FRR (54.4–69.3%) to increase. After three cycles, regeneration capability was enhanced from 45.1 to 57.9%.	[81]
PVC (UF)	Boehmite (30 nm)	NIPS	71.3–57.2	500 ppm BSA solution	Pore size (from 11.1 to 14.9 nm.), hydraulic permeability (211.3–350.7 L/m^2.h.bar), and FRR (from 44.3 to 60.4%) were improved by the addition of nanoparticles. At the end of the 4th regeneration cycles, water flux recovery improved from 20.6 to 47.7%.	[82]
PVDF (UF)	TiO_2/GO	NIPS	66–53	1000 ppm BSA solution	With the increased in pore size (50–57.6 nm.) and hydrophilicity, hydraulic permeability from37.9 to 200 L/m^2.h.bar. and FRR from 51.1 to 89.2% were increased.	[83]
PVDF (UF)	Vermiculate 82 nm CuO <50 nm Al_2O_3 < 50 nm SiO_2 < 200 nm	NIPS	82.6–57.3 66.4 62.5 64.8	1000 ppm BSA solution pH 7	Humic acid (HA) rejection (94.6, 88.3, 91.7, and 89%) and hydraulic permeability (444, 372.9, 425.7, and 405.7 L/m^2.h.bar) and stability at the end of 4th regeneration cycles (81.5, 61.4, 73.8, and 68.3%) were improved when vermiculate, cuprous oxide, alumina, and silica was added respectively. The properties of the neat membrane were reported as 80.9% HA rejection, 367.3 L/m^2.h.bar. Hydraulic permeability, and 45.5% water flux recovery at the end of 4th cycles.,	[84]
PSf (UF)	GO nanosheets	NIPS	94–83.3	200 ppm BSA solution	Hydraulic permeability and pore size increased from 98 to 294 L/m^2.h.bar. and from 19 to 31 nm., while rejection was unchanged. After two cycles, water flux recovery enhanced from 73.4 to 82.4%.	[85]

Table 2.
Filtration performances and physical characteristics of the hybrid membranes prepared by blending method.

to the hydrogen bonding force and more electrostatic repulsion properties of $sTiO_2$ NPs. The same group has also investigated the effect of the addition of sulfonated graphene oxide (sGO) NPs into PVDF membranes fabricated by the phase inversion method [89]. A gradual increase in water fluxes was obtained up to the sGO loading concentration of 0.8% meaning to the elimination of aggregation. Maximum water permeability attained at the 0.8 wt% of sGO addition was reported as 146% higher than the neat PVDF. The enhancement of the water flux has been explained by the improved charge density due to the availability of extra sulfonic groups on sGO supports that can attract more water layer. In addition, the attached $–SO_3H$ group in sGO provides stronger hydrogen-bonding with respect to –OH/-COOH groups available in native GO. The performances of the CNT and sulfonated CNT (sCNT) NPs blended PVDF UF membranes were compared for the objective of conserving the bacterial population and providing antifouling property [90]. The porosity, pore size, water flux, fouling recovery ratio values of PVDF-CNT and PVDF-sCNT were obtained as 81 and 84%, 50 and 60 nm, 360 and 680 $L/m_2.h$ and 72.7 and 83.5%, respectively. In addition, the BSA (bovine serum albumin) rejection was 90% in the PVDF-sCNT. Authors demonstrated that the fabricated composite membranes were nontoxic to the bacterial population, hence the proposed membrane architecture can be a promising approach for membrane bioreactor systems in wastewater treatment plants.

4. Conclusion

Membranes containing nanomaterials in the form of MMNMs or TFN, ensure outstanding features in terms of permeability, selectivity, antifouling, and self-cleaning ability for water applications due to their synergistic effects. However, there are still major challenges to developing high-performance membranes for large scale water treatments. Difficulties in dispersion of inorganic nanoparticles in a polymer matrix, the release of nanoparticles and associated environmental toxicity, long term stability, and the production cost of the nanocomposite membrane, needs to be further explored. Care should be taken that the nanoparticles selected do not sacrifice an ability of the membranes to improve another ability.

Conflict of interest

The author declares no conflict of interest.

Author details

Yilmaz Yurekli
Engineering Faculty, Bioengineering Department, Manisa Celal Bayar University, Manisa, Turkey

*Address all correspondence to: yilmazyurekli@gmail.com

References

[1] XueMei Tan, Denis Rodrigue, A Review on Porous Polymeric Membrane Preparation. Part I: Production Techniques with Polysulfone and Poly (Vinylidene Fluoride), Polymers 11 (2019) 1160.

[2] Z. Xu, T. Wu, J. Shi, W. Wang, K. Teng, X. Qian, M. Shan, H. Deng, X. Tian, C. Li, F. Li, Manipulating Migration Behavior of Magnetic Graphene Oxide via Magnetic Field Induced Casting and Phase Separation toward High Performance Hybrid Ultrafiltration Membranes, ACS Applied Materials & Interfaces, 8 (2016) 18418-18429.

[3] Z. Xu, T. Wu, J. Shi, K. Teng, W. Wang, M. Ma, J. Li, X. Qian, C. Li, J. Fan, Photocatalytic antifouling PVDF ultrafiltration membranes based on synergy of graphene oxide and TiO2 for water treatment, J. Membr. Sci., 520 (2016) 281-293.

[4] Jun Yin, Baolin Deng , Polymer-matrix nanocomposite membranes for water treatment, Journal of Membrane Science 479 (2015)256-275.

[5] Meenakshi Sundaram Sri Abirami Saraswathi, Alagumalai Nagendran, Dipak Rana, Tailored polymer nanocomposite membranes based on carbon, metal oxide and silicon nanomaterials: a review, J. Mater. Chem. A 7 (2019) 8723-8745.

[6] Li-guang Wu, Xue-yang Zhang, Ting Wang, Chun-hui Du, Cai-hong Yang, Enhanced performance of polyvinylidene fluoride ultrafiltration membranes by incorporating TiO_2/graphene oxide, Chemical Engineering Research and Design 141 (2019) 492-501.

[7] Shujuan Yang, Qinfeng Zou, Tianhao Wang, Liping Zhang, Effects of GO and MOF@GO on the permeation and antifouling properties of cellulose acetate ultrafiltration membrane, Journal of Membrane Science 569 (2019) 48-59.

[8] Luo M.L., Zhao J.Q., Tang W., Pu C.S., Hydrophilic modification of poly (ether sulfone) ultrafiltration membrane surface by self-assembly of TiO2 nanoparticles, Appl. Surf. Sci.1 (2005) 76-84.

[9] Li X., Li J., Van der Bruggen B., Sun X., Shen J., Han W., Wang L., Fouling behavior of polyethersulfone ultrafiltration membranes functionalized with sol–gel formed ZnO nanoparticles, RSC Adv. 63 (2015) 50711-50719.

[10] Zhu X., Bai R., Wee K.H., Liu C., Tang S.L., Membrane surfaces immobilized with ionic or reduced silver and their anti-biofouling performances, J. Membr. Sci. 1 (2010) 278-286.

[11] Yin J., Kim E.S., Yang J., Deng B., Fabrication of a novel thin-film nanocomposite (TFN) membrane containing MCM-41 silica nanoparticles (NPs) for water purification, J. Membr. Sci. 423 (2012) 238-246.

[12] Mendez R., Constant B., Garzon C., Nisar M., Nachtigall S.M.B., Quijada R., Barrier, mechanical and conductive properties of polycaprolactam nanocomposites containing carbon-based particles: Effect of the kind of particle, Polymer 130 (2017) 10-16.

[13] Hassan M., Reddy K.R., Haque E., Faisal S.N., Ghasemi S., Minett A.I., Gomes V.G., Hierarchical assembly of graphene/polyaniline nanostructures to synthesize freestanding supercapacitor electrode, Compos. Sci. Technol. 98 (2014) 1-8.

[14] Homayoonfal M., Mehrnia M.R., Niassar M.S., Akbari A.,

Sarrafzadeh M.H., Ismail A.F., Fabrication of magnetic nanocomposite membrane for separation of organic contaminant from water, Desalin. Water Treat. 54 (2015) 3603-3609.

[15] C. Zhao, X. Xu, J. Chen, G. Wang, F. Yang, Highly effective antifouling performance of PVDF/graphene oxide composite membrane in membrane bioreactor (MBR) system, Desalination 340 (2014) 59-66.

[16] Robertson, J.M.C., Robertson, P.K.J., Lawton, L.A., 2005. A comparison of the effectiveness of TiO2 photocatalysis and UVA photolysis for the destruction of three pathogenic microorganisms. J. Photochem. Photobiol. A: Chem. 175, 51-56.

[17] Skorb, E.V., Antonouskaya, L.I., Belyasova, N.A., Shchukin, D.G., Mohwald, H., Sviridov, D.V., 2008. Antibacterial activity of thin-film photocatalysts based on metal-modified TiO2 and TiO2:In2O3 nanocomposite. Appl. Catal. B: Environ. 84, 94-99.

[18] A. Charkhia, M. Kazemeinia, S.J. Ahmadib, H. Kazemian, Fabrication ofgranulated NaY zeolite nanoparticles using a new method and study theadsorption properties, Powder Technol. 231 (2012) 1-6.

[19] Y. Wang, Z. Lei, B. Chen, Q. Guo, N. Liu, Adsorption of NO and N2O on Fe-BEAand H-BEA zeolites, Appl. Surf. Sci. 256 (2010) 4042-4047.

[20] S. Malamisa, E. Katsoua, A review on zinc and nickel adsorption on naturaland modified zeolite, bentonite and vermiculite: examination of processparameters, kinetics and isotherms, J. Hazard. Mater. 252-253 (252) (2013)428-461.

[21] Fang X., Li J., Ren B., Huang Y., Wang D., Liao Z., Li Q., Wang L., Dionysiou D.D., 2019, Polymeric ultrafiltration membrane with in situ formed nano-silver within the inner pores for simultaneous separation and catalysis, J. Membr. Sci., 579, 190-198

[22] Choi W., Choi J., Bang J., Lee J.H., 2013, Layer-by-Layer Assembly of Graphene Oxide Nanosheets on Polyamide Membranes for Durable Reverse-Osmosis Applications, ACS Appl. Mater. Interfaces, 52, 3, 12510-12519

[23] Lau W., Gray S., Matsuura T., Emadzadeh D., Chen J.P., Ismail A, 2015, A review on polyamide thin film nanocomposite (TFN) membranes: history, applications, challenges and approaches, Water Res., 80, 306-324.

[24] Liang S., Xiao K., Zhang S., Ma Z., Lu P., Wang H., Huang X., 2018, A facile approach to fabrication of superhydrophilic ultrafiltration membranes with surface-tailored nanoparticles, Sep. Purif. Technol., 203, 251-259.

[25] Ko K., Yu Y.J., Kim M.J., Kweon J., Chun H., 2018, Improvement in fouling resistance of silver-graphene oxide coated polyvinylidene fluoride membrane prepared by pressurized filtration, Sep. Purif. Technol., 194, 161-169.

[26] Cheng X., Zhou W., Li P., Ren Z., Wu D., Luo C., Tang X., Wang J., Liang H., 2019, Improving ultrafiltration membrane performance with pre-deposited carbon nanotubes/ nanofibers layers for drinking water treatment, Chemosphere, 234, 545-557.

[27] Mou Paul, Steven D. Jons, Chemistry and fabrication of polymeric nanofiltration membranes: A review, Polymer 103 (2016) 417-456.

[28] Filiz Yasar Mahlicli, Sacide Alsoy Altinkaya, Yilmaz Yurekli, Preparation and characterization of polyacrylonitrile membranes modified

with polyelectrolyte deposition for separating similar sized proteins, Journal of Membrane Science 415-416 (2012) 383-390.

[29] Nithya Joseph, Pejman Ahmadiannamini, Richard Hoogenboom, Ivo. F. J. Vankelecom, Layer-by-layer preparation of polyelectrolyte multilayer membranes for separation, *Polym. Chem.* 5 (2014) 1817-1831

[30] Bartosz Czerwieniec, Marcin Strawski, Ludomira H. Granicka, Marek Szklarczyk, AFM study of adhesion and interactions between polyelectrolyte bilayers assembly, Colloids and Surfaces A: Physicochemical and Engineering Aspects 555 (2018) 465-472

[31] Joseph J. Richardson, Mattias Björnmalm, Frank Caruso, Technology-driven layer-by-layer assembly of nanofilms, Science, 348 (2015) 2491.

[32] Salomäki, M., Vinokurov, I.A. & Kankare, J. (2005) Effect of temperature on the buildup of polyelectrolyte multilayers. Langmuir, 21, 11,232-11,240.

[33] R.H. Lajimi, et al., Change of the performance properties of nanofiltration cellulose acetate membranes by surface adsorption of polyelectrolyte multilayers, Desalination 163 (1-3) (2004) 193-202.

[34] Kolarik, L., Furlong, D.F., Joy, H., Struijk, C. & Rowe, R. (1999) Building assemblies from high molecular weight polyelectrolytes. Langmuir, 15, 8265-8275.

[35] Önder Tekinalp, Sacide Alsoy Altinkaya, Development of high flux nanofiltration membranes through single bilayer polyethyleneimine/ alginate deposition, Journal of Colloid and Interface Science, 537 (2019) 215-227

[36] S.T. Dubas, J.B. Schlenoff, Swelling and smoothing of polyelectrolyte multilayers by salt, Langmuir 17 (2001) 7725-7727.

[37] N.G. Hoogeveen, M.A.C. Stuart, G.J. Fleer, Polyelectrolyte adsorption on oxides.2. Reversibility and exchange, J. Colloid Interface Sci. 182 (1996) 146-157.

[38] Schlenoff, J.B., Rmaile, A.H. & Bucur, C.B. (2008) Hydration contributions to association in polyelectrolyte multilayers and complexes: visualizing hydrophobicity. Journal of the American Chemical Society, 130, 13589-13597.

[39] Qing Chen, Pingping Yu, Wenqiang Huang, Sanchuan Yu, Meihong Liu, Congjie Gao, High-flux composite hollow fiber nanofiltration membranes fabricated through layer-by-layer deposition of oppositely charged crosslinked polyelectrolytes for dye removal, Journal of Membrane Science, 492, (2015), 312 321.

[40] Glinel, K., Moussa, A., Jonas, A.M. & Laschewsky, A. (2002) Influence of polyelectrolyte charge density on the formation of multilayers of strong polyelectrolytes at low ionic strength. Langmuir, 18, 1408-1412.

[41] Wang, J., Yao, Y., Yue, Z. & Economy, J. (2009) Preparation of polyelectrolyte multilayer films consisting of sulfonated poly (ether ether ketone) alternating with selected anionic layers. Journal of Membrane Science, 337, 200-207.

[42] Guillaume-Gentil, O., Zahn, R., Lindhoud, S., Graf, N., Voros, J. & Zambelli, T. (2011) From nanodroplets to continuous films: how the morphology of polyelectrolyte multilayers depends on the dielectric permittivity and the surface charge of the supporting substrate. Soft Matter, 7, 3861-3871.

[43] Merry Sianipar, Seung Hyun Kim, Khoiruddin, Ferry Iskandar, Gede Wenten, Functionalized carbon nanotube (CNT) membrane: progress and challenges, RSC Adv., 2017, 7, 51175.

[44] H. Zarrabi, M. E. Yekavalangi, V. Vatanpour, A. Shockravi and M. Safarpour, Desalination, 2016, 394, 83-90.

[45] S.-M. Xue, Z.-L. Xu, Y.-J. Tang and C.-H. Ji, ACS Appl. Mater. Interfaces, 2016, 8, 19135-19144.

[46] H. Wu, B. Tang, P. Wu, Optimizing polyamide thin film composite membrane covalently bonded with modified mesoporous silica nanoparticles, J. Membr. Sci. 428 (2013) 341-348.

[47] F. Perreault, M.E. Tousley, M. Elimelech, Thin-film composite polyamide membranes functionalized with biocidal graphene oxide nanosheets, Environ. Sci.Technol. Lett. 1 (2013) 71-76

[48] J. Yin, G. Zhu, B. Deng, Graphene oxide (GO) enhanced polyamide (PA) thin-film nanocomposite (TFN) membrane for water purification, Desalination 379 (2016) 93-101.

[49] J. Wang, Y. Wang, Y. Zhang, A. Uliana, J. Zhu, J. Liu, B. Van der Bruggen, Zeolitic imidazolate framework/graphene oxide hybrid nanosheets functionalized thin film nanocomposite membrane for enhanced antimicrobial performance, ACS Appl. Mater. Interfaces 8 (2016) 25508-25519.

[50] S. Pourjafar, A. Rahimpour, M. Jahanshahi, Synthesis and characterization of PVA/PES thin film composite nanofiltration membrane modified with TiO2 nanoparticles for better performance and surface properties, J. Ind. Eng. Chem. 18 (2012) 1398-1405.

[51] S. Zhao, Z. Wang, A loose nano-filtration membrane prepared by coating HPAN UF membrane with modified PEI for dye reuse and desalination, J. Membr. Sci. 524 (2017) 214-224.

[52] S.F. Seyedpour, A. Rahimpour, H. Mohsenian, M.J. Taherzadeh, Low fouling ultrathin nanocomposite membranes for efficient removal of manganese, J. Membr. Sci. (2017).

[53] Qing Chen, Pingping Yu, Wenqiang Huang, Sanchuan Yu, Meihong Liu, Congjie Gao, High-flux composite hollow fiber nanofiltration membranes fabricated through layer-by-layer deposition of oppositely charged crosslinked polyelectrolytes for dye removal, Journal of Membrane Science 492 (2015) 312-321.

[54] Yuchuan Liu, Zongxue Yu, Xiuhui Li, Liangyan Shao, Haojie Zeng, Super hydrophilic composite membrane with photocatalytic degradation and self-cleaning ability based on LDH and g-C3N4, Journal of Membrane Science 617 (2021) 118504.

[55] M.-B. Wu, Y. Lv, H.-C. Yang, L.-F. Liu, X. Zhang and Z.-K. Xu, J. Membr. Sci., 2016, 515, 238-244.

[56] J. Zhao, Y. Zhu, F. Pan, G. He, C. Fang, K. Cao, R. Xing and Z. Jiang, J. Membr. Sci., 2015, 487, 162-172.

[57] X. Song, R. S. Zambare, S. Qi, B. N. I. L. Sowrirajalu, A.P. James Selvaraj, C. Y. Tang and C. Gao, ACS Appl.Mater. Interfaces, 2017, 9, 41482-41495.

[58] M. Hu and B. Mi, Environ. Sci. Technol., 2013, 47, 3715-3723.

[59] Xin-Yu Gong, Zhi-Hao Huang, Hao Zhang, Wei-Liang Liu, Xiao-Hua Ma, Zhen-Liang Xu, Novel high-flux positively charged composite membrane incorporating titanium-based MOFs

for heavy metal removal, Chemical Engineering Journal 398 (2020) 125706.

[60] A. Sotto, A. Boromand, R. Zhang, P. Luis, J.M. Arsuaga, J. Kim, B. Van der Bruggen, Effect of nanoparticle aggregation at low concentrations of TiO2 on the hydrophilicity, morphology, and fouling resistance of PES–TiO2 membranes, J. Colloid Interface Sci. 363 (2011) 540-550.

[61] N.Abdullah, N.Yusof, A.F.Ismail, W.J.Lau, Insights into metal-organic frameworks-integrated membranes for desalination process: A review, Desalination 500 (2021) 114867.

[62] B. Zornoza, C. Tellez, J. Coronas, J. Gascon, F. Kapteijn, Metal organic framework based mixed matrix membranes: an increasingly important field of research with a large application potential, Microporous Mesoporous Mater. 166 (2013) 67-78.

[63] Ze Xian Low, Amir Razmjou, Kun Wang, Stephen Gray, Mikel Duke, Huanting Wang, Effect of addition of two-dimensional ZIF-L nanoflakes on the properties of polyethersulfone ultrafiltration membrane, Journal of Membrane Science, 460, (2014) 9-17.

[64] C. Wang, X. Liu, J.P. Chen, K. Li, Superior removal of arsenic from water with zirconium metal-organic framework UiO-66, Sci. Rep. 5 (2015) 16613.

[65] A. Abbasi, T. Moradpour, K. Van Hecke, A new 3D cobalt (II) metal–organic framework nanostructure for heavy metal adsorption, Inorganica Chim. Acta 430 (2015) 261-267.

[66] Sana Jamshidifard, Shahnaz Koushkbaghi, Seyedehgolshan Hosseini, Sina Rezaei, Alireza Karamipour, Azadeh Jafari rad, Mohammad Iran, Incorporation of UiO-66-NH2 MOF into the PAN/chitosan nanofibers for adsorption and membrane filtration of Pb(II), Cd(II) and Cr(VI) ions from aqueous solutions, Journal of Hazardous Materials, 368 (2019) 10-20.

[67] Y. Yurekli, Removal of heavy metals in wastewater by using zeolite nano-particles impregnated polysulfone membranes, J. Hazard. Mater. 309(2016) 53-64.

[68] S.M. Hosseini, S. Rafiei, A.R. Hamidi, A.R. Moghadassi, S.S. Madaeni, Preparation and electrochemical characterization of mixed matrix heterogeneous cation exchange membranes filled with zeolite nanoparticles: ionic transport property in desalination, Desalination 351 (2014) 138-144.

[69] Mukherjee R, Bhunia P, De S (2016) Impact of graphene oxide on removal of heavy metals using mixed matrix membrane. Chem Eng J 292:284-297.

[70] Subramaniam M.N., Goh P.S., Lau W.J., Tan Y.H., Ng B.C., Ismail A.F., 2017, Hydrophilic hollow fiber PVDF ultrafiltration membrane incorporated with titanate nanotubes for decolourization of aerobically-treated palm oil mill effluent, Chem. Eng. J. 316, 101-110.

[71] Yan L., Li Y.S., Xiang C.B., 2005, Preparation of poly (vinylidene fluoride)(pvdf) ultrafiltration membrane modified by nano-sized alumina (Al2O3) and its antifouling research, Polymer, 46, 7701-7706.

[72] Maximous N., Nakhla G., Wan W., Wong K., 2009, Preparation, characterization and performance of Al2O3/PES membrane for wastewater filtration, J. Membr. Sci., 341, 67-75.

[73] Gholami F., Zinadini S., Zinatizadeh A. A., Abbasi A. R., 2018, TMU-5 Metal-Organic frameworks (MOFs) as a novel nanofiller for flux increment and fouling mitigation in PES

ultrafiltration membrane, Sep. Purif. Technol., 194, 272-280.

[74] Xiao Y.T., Xu C.X., Geng H.Z., Ji Q., Wang L., He B., Jiang Y., Kong J., Lia J., 2020, Multifunctional PVDF/CNT/GO Mixed Matrix Membranes for Ultrafiltration 1and Fouling Detection, J. Hazard. Mater., 384, 120978.

[75] Liang S., Xiao K., Zhang S., Ma Z., Lu P., Wang H., Huang X., 2018, A facile approach to fabrication of superhydrophilic ultrafiltration membranes with surface-tailored nanoparticles, Sep. Purif. Technol., 203, 251-259.

[76] Zhou J., Sun D., Wang L., Guo L., Chen W., Yu F., Wang Y., Yang Y., 2019, Two-dimensional superstructures filled into polysulfone membranes for highly improved ultrafiltration: The case of cuprous iodide nanosheets, J. Membr. Sci., 576, 142-149.

[77] Nasrollahi N., Aber S., Vatanpour V., Mahmoodi N.M., 2019, Development of hydrophilic microporous PES ultrafiltration membrane containing CuO nanoparticles with improved antifouling and separation performance, Mater. Chem. Phys., 222, 338-350.

[78] Yang S., Zou Q., Wang T., Zhang L., 2019, Effects of GO and MOF@GO on the permeation and antifouling properties of cellulose acetate ultrafiltration membrane, J. Membr. Sci., 569, 48-59.

[79] Liu Q., Huang S., Zhang Y., Zhao S., 2018, Comparing the antifouling effects of activated carbon and TiO_2 in ultrafiltration membrane development, J. Colloid Interf. Sci., 515, 109-118.

[80] Jiang Y., Zeng Q., Biswas P., Fortner J.D., 2019, Graphene oxides as nanofillers in polysulfone ultrafiltration membranes: Shape matters, J. Membr. Sci., 581, 453-461.

[81] Mu Y., Zhu K., Luan J., Zhang S., Zhang C., Na R., Yang Y., Zhang X., Wang G., 2019, Fabrication of hybrid ultrafiltration membranes with improved water separation properties by incorporating environmentally friendly taurine modified hydroxyapatite nanotubes, J. Membr. Sci., 577, 274-284.

[82] Farjami M., Moghadassi A., Vatanpour V., Hosseini S.M., Parvizian F., 2019, Preparation and characterization of a novel high-flux emulsion polyvinyl chloride (EPVC) ultrafiltration membrane incorporated with boehmite nanoparticles, J. Ind. Eng. Chem., 72, 144-156.

[83] Wu L.G., Zhang X.Y., Wang T., Du C.H, Yang C.H., 2019, Enhanced performance of polyvinylidene fluoride ultrafiltration membranes by incorporating TiO2/graphene oxide, Chem. Eng. Res. Des., 141, 492-501.

[84] Isawi H., 2019, Evaluating the performance of different nano-enhanced ultrafiltration membranes for the removal of organic pollutants from wastewater, J.Water Process Eng., 31, 100833.

[85] Zhang G., Zhou M., Xu Z., Jiang C., Shen C., Meng Q., 2019, Guanidyl-functionalized graphene/polysulfone mixed matrix ultrafiltration membrane with superior permselective, antifouling and antibacterial properties for water treatment, J. Colloid Interf. Sci., 540, 295-305.

[86] Pendergast M.T.M., Nygaard J.M., Ghosh A.K., Hoek E.M., 2010, Using nanocomposite materials technology to understand and control reverse osmosis membrane compaction, Desalination, 261, 255-263.

[87] Heinz H., Pramanik C., Heinz O., Ding Y., Mishra R.K., Marchon D., Flatt R.J., Lopis I.E., Llop J., Moya S., Ziolo R.F., 2017, Nanoparticle decoration with surfactants: Molecular interactions,

assembly, and applications, Surf. Sci. Rep., 72, 1-58.

[88] Ayyaru S., Ahn Y.H., 2018, Fabrication and separation performance of polyethersulfone/ sulfonated TiO2 (PES–STiO2) ultrafiltration membranes for fouling mitigation, J. Ind. Eng. Chem., 67, 199-209.

[89] Ayyaru S., Ahn Y.H., 2017, Application of sulfonic acid group functionalized graphene oxide to improve hydrophilicity, permeability, and antifouling of PVDF nanocomposite ultrafiltration membrane, J. Membr. Sci., 525, 210-219.

[90] Ayyaru S., Pandiyan R., Ahn Y.H., 2019, Fabrication and characterization of anti-foulingand non-toxic polyvinylidene fluoride-Sulphonated carbon nanotube ultrafiltration membranes for membrane bioreactors applications, Chem. Eng. Res. Des., 142, 176-188.